

Pion Photo- and Electroproduction and the Chiral MAID Interface

Marius HILT¹, Björn C. LEHNHART¹, Stefan SCHERER¹, and Lothar TIATOR¹

¹*PRISMA Cluster of Excellence, Institut für Kernphysik, Johannes Gutenberg-Universität Mainz, D-55099 Mainz, Germany*

E-mail: scherer@kph.uni-mainz.de

(Received October 16, 2015)

We discuss the extended on-mass-shell scheme for manifestly Lorentz-invariant baryon chiral perturbation theory. We present a calculation of pion photo- and electroproduction up to and including order q^4 . The low-energy constants have been fixed by fitting experimental data in all available reaction channels. Our results can be accessed via a web interface, the so-called chiral MAID (<http://www.kph.uni-mainz.de/MAID/chiralmid/>).

KEYWORDS: chiral perturbation theory, pion photoproduction, pion electroproduction

1. Introduction

In the middle of the 1980s, renewed interest in neutral pion photoproduction at threshold was triggered by experimental data from Saclay and Mainz [1, 2], which indicated a serious disagreement with the predictions for the s -wave electric dipole amplitude E_{0+} based on current algebra and PCAC [3–5]. This discrepancy was explained with the aid of chiral perturbation theory (ChPT) [6]. Pion loops, which are beyond the current-algebra framework, generate infrared singularities in the scattering amplitude which then modify the predicted low-energy expansion of E_{0+} (see also Ref. [7]). Subsequently, several experiments investigating pion photo- and electroproduction in the threshold region were performed at Mainz, MIT-Bates, NIKHEF, Saskatoon and TRIUMF, and on the theoretical side, all of the different reaction channels of pion photo- and electroproduction near threshold were extensively investigated by Bernard, Kaiser, and Meißner within the framework of heavy-baryon chiral perturbation theory (HBChPT) [8]. For a complete list of references, see Ref. [9]. In the beginning, the manifestly Lorentz-invariant or relativistic formulation of ChPT (RChPT) was abandoned, as it seemingly had a problem with respect to power counting when loops containing internal nucleon lines come into play. In the meantime, the development of the infrared regularization (IR) scheme [10] and the extended on-mass-shell (EOMS) scheme [11, 12] offered a solution to the power-counting problem, and RChPT became popular again.

Here, we give a short introduction to the EOMS scheme and present its application to a calculation of pion photo- and electroproduction up to and including order q^4 [$\mathcal{O}(q^4)$]. We present the so-called chiral MAID (χ MAID) [13] which provides the numerical results of these calculations.

2. Renormalization and Power Counting

ChPT is the effective field theory of QCD in the low-energy regime [14–16] (for an introduction, see Refs. [17, 18]). The prerequisite for an effective field theory program is (a) a knowledge of the most general effective Lagrangian and (b) an expansion scheme for observables in terms of a consistent power counting method.

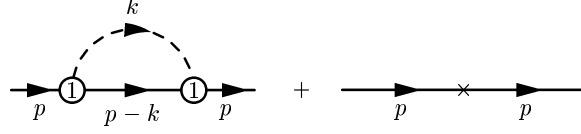


Fig. 1. Renormalized one-loop self-energy diagram. The number 1 in the interaction blobs refers to $\mathcal{L}_{\pi N}^{(1)}$. The cross generically denotes counter-term contributions.

2.1 Effective Lagrangian and Power Counting

The effective Lagrangian relevant to the one-nucleon sector consists of the sum of the purely mesonic and πN Lagrangians, respectively,

$$\mathcal{L}_{\text{eff}} = \mathcal{L}_{\pi} + \mathcal{L}_{\pi N} = \mathcal{L}_{\pi}^{(2)} + \mathcal{L}_{\pi}^{(4)} + \dots + \mathcal{L}_{\pi N}^{(1)} + \mathcal{L}_{\pi N}^{(2)} + \dots,$$

which are organized in a derivative and quark-mass expansion [14–16]. For example, the lowest-order basic Lagrangian $\mathcal{L}_{\pi N}^{(1)}$, already expressed in terms of renormalized parameters and fields, is given by

$$\mathcal{L}_{\pi N}^{(1)} = \bar{\Psi} (i\gamma_{\mu}\partial^{\mu} - m) \Psi - \frac{1}{2} \frac{g_A}{F} \bar{\Psi} \gamma_{\mu} \gamma_5 \tau^a \partial^{\mu} \pi^a \Psi + \dots, \quad (1)$$

where m , g_A , and F denote the chiral limit of the physical nucleon mass, the axial-vector coupling constant, and the pion-decay constant, respectively. The ellipsis refers to terms containing external fields and higher powers of the pion fields. When studying higher orders in perturbation theory, one encounters ultraviolet divergences. As a preliminary step, the loop integrals are regularized, typically by means of dimensional regularization. In the process of renormalization the counter terms are adjusted such that they absorb all the ultraviolet divergences occurring in the calculation of loop diagrams [19]. This will be possible, because we include in the Lagrangian all of the infinite number of interactions allowed by symmetries [20]. When renormalizing, we still have the freedom of choosing a renormalization prescription. In this context the finite pieces of the renormalized couplings will be adjusted such that renormalized diagrams satisfy the following power counting: a loop integration in n dimensions counts as q^n , pion and nucleon propagators count as q^{-2} and q^{-1} , respectively, vertices derived from $\mathcal{L}_{\pi}^{(2k)}$ and $\mathcal{L}_{\pi N}^{(k)}$ count as q^{2k} and q^k , respectively. Here, q collectively stands for a small quantity such as the pion mass, small external four-momenta of the pion, and small external three-momenta of the nucleon. The power counting does not uniquely fix the renormalization scheme, i.e., there are different renormalization schemes such as the IR [10] and EOMS [11, 12] schemes, leading to the above specified power counting.

2.2 Example: One-Loop Contribution to the Nucleon Mass

In the mesonic sector, the combination of dimensional regularization and the modified minimal subtraction scheme $\overline{\text{MS}}$ leads to a straightforward correspondence between the chiral and loop expansions [15]. By discussing the one-loop contribution of Fig. 1 to the nucleon self energy, we will see that this correspondence, at first sight, seems to be lost in the baryonic sector. According to the power counting specified above, after renormalization, we would like to have the order $D = n \cdot 1 - 2 \cdot 1 - 1 \cdot 1 + 1 \cdot 2 = n - 1$. An explicit calculation yields [18]

$$\Sigma_{\text{loop}} = -\frac{3g_A^2}{4F^2} \left\{ (\not{p} + m)I_N + M^2(\not{p} + m)I_{N\pi} - \frac{(p^2 - m^2)\not{p}}{2p^2} [(p^2 - m^2 + M^2)I_{N\pi} + I_N - I_{\pi}] \right\},$$

where $M^2 = 2B\hat{m}$ is the lowest-order expression for the squared pion mass in terms of the low-energy coupling constant B and the average light-quark mass \hat{m} [15]. The relevant loop integrals are defined

as

$$I_\pi = \mu^{4-n} \int \frac{d^n k}{(2\pi)^n} \frac{i}{k^2 - M^2 + i0^+}, \quad I_N = \mu^{4-n} \int \frac{d^n k}{(2\pi)^n} \frac{i}{k^2 - m^2 + i0^+}, \quad (2)$$

$$I_{N\pi} = \mu^{4-n} \int \frac{d^n k}{(2\pi)^n} \frac{i}{[(k-p)^2 - m^2 + i0^+]} \frac{1}{k^2 - M^2 + i0^+}. \quad (3)$$

The application of the $\widetilde{\text{MS}}$ renormalization scheme of ChPT [15, 16]—indicated by “r”—yields

$$\Sigma_{\text{loop}}^r = -\frac{3g_{Ar}^2}{4F_r^2} [M^2(\not{p} + m)I_{N\pi}^r + \dots].$$

The expansion of $I_{N\pi}^r$ is given by

$$I_{N\pi}^r = \frac{1}{16\pi^2} \left(-1 + \frac{\pi M}{m} + \dots \right),$$

resulting in $\Sigma_{\text{loop}}^r = O(q^2)$. In other words, the $\widetilde{\text{MS}}$ -renormalized result does not produce the desired low-energy behavior which, for a long time, was interpreted as the absence of a systematic power counting in the relativistic formulation of ChPT.

The expression for the nucleon mass m_N is obtained by solving the equation

$$m_N - m - \Sigma(m_N) = 0,$$

from which we obtain for the nucleon mass in the $\widetilde{\text{MS}}$ scheme [16],

$$m_N = m - 4c_{1r}M^2 + \frac{3g_{Ar}^2M^2}{32\pi^2F_r^2}m - \frac{3g_{Ar}^2M^3}{32\pi F_r^2}. \quad (4)$$

At $O(q^2)$, Eq. (4) contains, besides the undesired loop contribution proportional to M^2 , the tree-level contribution $-4c_{1r}M^2$ from the next-to-leading-order Lagrangian $\mathcal{L}_{\pi N}^{(2)}$.

The solution to the power-counting problem is the observation that the term violating the power counting, namely, the third on the right-hand side of Eq. (4), is *analytic* in the quark mass and can thus be absorbed in counter terms. In addition to the $\widetilde{\text{MS}}$ scheme we have to perform an additional *finite* renormalization. For that purpose we rewrite

$$c_{1r} = c_1 + \delta c_1, \quad \delta c_1 = \frac{3mg_A^2}{128\pi^2F_r^2} + \dots \quad (5)$$

in Eq. (4) which then gives the final result for the nucleon mass at $O(q^3)$:

$$m_N = m - 4c_1M^2 - \frac{3g_A^2M^3}{32\pi F^2}. \quad (6)$$

We have thus seen that the validity of a power-counting scheme is intimately connected with a suitable renormalization condition. In the case of the nucleon mass, the $\widetilde{\text{MS}}$ scheme alone does not suffice to bring about a consistent power counting.

2.3 Extended On-Mass-Shell Scheme

We illustrate the underlying ideas of the EOMS scheme in terms of a typical one-loop integral in the chiral limit,

$$H(p^2, m^2; n) = -i \int \frac{d^n k}{(2\pi)^n} \frac{1}{[(k-p)^2 - m^2 + i0^+][k^2 + i0^+]},$$

where $\Delta = (p^2 - m^2)/m^2 = O(q)$ is a small quantity. Applying the dimensional counting analysis of Ref. [21], the result of the integration is of the form

$$H \sim F(n, \Delta) + \Delta^{n-3} G(n, \Delta),$$

where F and G are hypergeometric functions which are analytic for $|\Delta| < 1$ for any n . The central idea of the EOMS scheme [11, 12] consists of subtracting those terms which violate the power counting as $n \rightarrow 4$. Since the terms violating the power counting are analytic in small quantities, they can be absorbed by counter-term contributions. In the present case, we want the renormalized integral to be of the order $D = n - 1 - 2 = n - 3$. To that end one first expands the integrand in small quantities and subtracts those integrated terms whose order is smaller than suggested by the power counting. The corresponding subtraction term reads [12]

$$H^{\text{subtr}} = -i \int \frac{d^n k}{(2\pi)^n} \frac{1}{[k^2 - 2p \cdot k + i0^+][k^2 + i0^+]} \Big|_{p^2=m^2} = \frac{m^{n-4}}{(4\pi)^{\frac{n}{2}}} \frac{\Gamma(2 - \frac{n}{2})}{n-3},$$

and the renormalized integral is written as

$$H^R = H - H^{\text{subtr}} = \frac{m^{n-4}}{(4\pi)^{\frac{n}{2}}} \left[-\Delta \ln(-\Delta) + (-\Delta)^2 \ln(-\Delta) + \dots \right] = O(q) \quad \text{as } n \rightarrow 4.$$

3. Pion Photo- and Electroproduction

3.1 Invariant Amplitude and Cross Section

In the one-photon-exchange approximation, the invariant amplitude for the reaction $e(k_i) + N(p_i) \rightarrow e(k_f) + N(p_f) + \pi(q)$ may be written as

$$\mathcal{M} = \epsilon_\mu \mathcal{M}^\mu, \quad \epsilon_\mu = e \frac{\bar{u}(k_f) \gamma_\mu u(k_i)}{k^2}, \quad k = k_i - k_f,$$

where ϵ_μ denotes the polarization vector of the virtual photon and \mathcal{M}^μ is the transition current matrix element: $\mathcal{M}^\mu = -ie \langle N(p_f), \pi(q) | J^\mu(0) | N(p_i) \rangle$. Using current conservation, $k_\mu \mathcal{M}^\mu = 0$, the transition current matrix element may be parameterized in terms of six invariant amplitudes A_i ,

$$\mathcal{M}^\mu = \bar{u}(p_f) \left(\sum_{i=1}^6 A_i(s, t, u) M_i^\mu \right) u(p_i), \quad (7)$$

where the Mandelstam variables s, t , and u satisfy $s + t + u = 2m_N^2 + M_\pi^2 - Q^2$ with $Q^2 = -k^2$. The M_i^μ are suitable, linearly independent 4×4 matrices such as, e.g.,

$$M_1^\mu = -\frac{i}{2} \gamma_5 (\gamma^\mu \not{k} - \not{k} \gamma^\mu), \quad \dots$$

For the purpose of performing a multipole expansion, we express the invariant amplitude in the center-of-mass (cm) frame as [22, 23]

$$\mathcal{M} = \frac{4\pi W}{m_N} \chi_f^\dagger \mathcal{F} \chi_i, \quad \chi: \text{Pauli spinor},$$

with the Chew-Goldberger-Low-Nambu (CGLN) amplitudes \mathcal{F}_i ($i = 1, \dots, 6$),

$$\mathcal{F} = i\vec{\sigma} \cdot \vec{d}_\perp \mathcal{F}_1(W, \Theta_\pi, Q^2) + \dots$$

The CGLN amplitudes can be expanded in a multipole series,

$$\mathcal{F}_1 = \sum_{l=0}^{\infty} \left\{ [lM_{l+} + E_{l+}] P'_{l+1}(x) + [(l+1)M_{l-} + E_{l-}] P'_{l-1}(x) \right\}, \quad \dots$$

where $x = \cos \Theta_\pi = \hat{q} \cdot \hat{k}$. Here, $P_l(x)$ is a Legendre polynomial of degree l , $P'_l = dP_l/dx$ and so on, with l denoting the orbital angular momentum of the pion-nucleon system in the final state. The multipoles $E_{l\pm}$, $M_{l\pm}$, and $L_{l\pm}$ are functions of the cm total energy W and the photon virtuality Q^2 and refer to transversal electric and magnetic transitions and longitudinal transitions, respectively. The subscript $l\pm$ denotes the total angular momentum $j = l \pm 1/2$ in the final state. Finally, in the isospin-symmetric limit, the four physical channels can be expressed in terms of three isospin amplitudes (0), (+), and (-):

$$\begin{aligned} A_i(\gamma^{(*)} p \rightarrow n\pi^+) &= \sqrt{2} (A_i^{(-)} + A_i^{(0)}), & A_i(\gamma^{(*)} n \rightarrow p\pi^-) &= -\sqrt{2} (A_i^{(-)} - A_i^{(0)}), \\ A_i(\gamma^{(*)} p \rightarrow p\pi^0) &= A_i^{(+)} + A_i^{(0)}, & A_i(\gamma^{(*)} n \rightarrow n\pi^0) &= A_i^{(+)} - A_i^{(0)}. \end{aligned}$$

For pion photoproduction with polarized photons from an unpolarized target without recoil polarization detection, the cross section can be written in the following way with the unpolarized cross section σ_0 and the photon beam asymmetry Σ .

$$\frac{d\sigma}{d\Omega} = \sigma_0 (1 - P_T \Sigma \cos 2\varphi). \quad (8)$$

For π^0 photoproduction on the proton, both observables are very precisely measured in the threshold region, allowing for an almost model independent partial wave analysis [24].

For pion electroproduction, in the one-photon-exchange approximation, the differential cross section can be written as

$$\frac{d\sigma}{d\mathcal{E}_f d\Omega_f d\Omega_\pi^{\text{cm}}} = \Gamma \frac{d\sigma_v}{d\Omega_\pi^{\text{cm}}}, \quad (9)$$

where Γ is the virtual photon flux and $d\sigma_v/d\Omega_\pi^{\text{cm}}$ is the pion production cross section for virtual photons.

For an unpolarized target and without recoil polarization detection, the virtual-photon differential cross section for pion production can be further decomposed as

$$\frac{d\sigma_v}{d\Omega_\pi} = \frac{d\sigma_T}{d\Omega_\pi} + \epsilon \frac{d\sigma_L}{d\Omega_\pi} + \sqrt{2\epsilon(1+\epsilon)} \frac{d\sigma_{LT}}{d\Omega_\pi} \cos \Phi_\pi + \epsilon \frac{d\sigma_{TT}}{d\Omega_\pi} \cos 2\Phi_\pi + h \sqrt{2\epsilon(1-\epsilon)} \frac{d\sigma_{LT'}}{d\Omega_\pi} \sin \Phi_\pi, \quad (10)$$

where it is understood that the variables of the individual virtual-photon cross sections $d\sigma_T/d\Omega_\pi$ etc. refer to the cm frame. For further details, especially concerning polarization observables, see Ref. [25].

3.2 Evaluation of the Invariant Amplitude and Chiral MAID

At $\mathcal{O}(q^3)$, the invariant amplitude involves 15 tree-level diagrams and 50 one-loop diagrams. At $\mathcal{O}(q^4)$, 20 tree-level diagrams and 85 one-loop diagrams contribute. We have calculated the loop contributions numerically, using the computer algebra system MATHEMATICA with the FeynCalc [26] and LoopTools packages [27]. We have explicitly verified that current conservation and crossing symmetry are fulfilled analytically for our results.

At $O(q^3)$, four independent LECs exist which are specifically related to pion photoproduction. Two of them enter the isospin $(-)$ channel and are, therefore, only relevant for the production of charged pions. Moreover, they contribute differently to the invariant amplitudes A_i of Eq. (7). The remaining two constants enter the isospin $(+)$ and (0) channels, respectively, though both in combination with the same Dirac structure. Finally, at $O(q^3)$ the description of pion electroproduction is a prediction, because no new parameter (LEC) beyond photoproduction is available at that order. At $O(q^4)$, 15 additional LECs appear. In the case of pion photoproduction, five constants contribute to the isospin (0) channel, five constants to the isospin $(+)$ channel, and one constant to the isospin $(-)$ channel. For electroproduction, the (0) and $(+)$ channels each have two more independent LECs. We note that the isospin $(-)$ channel, even at $O(q^4)$, does not contain any free LEC specifically related to electroproduction.

Figure 2 shows the homepage of the web interface chiral MAID. The loop contributions, including their parameters, are fixed and cannot be modified from the outside. On the other hand, the contact diagrams at $O(q^3)$ and $O(q^4)$ enter analytically and the corresponding LECs can be changed arbitrarily (see Ref. [9] for a discussion of our present values).

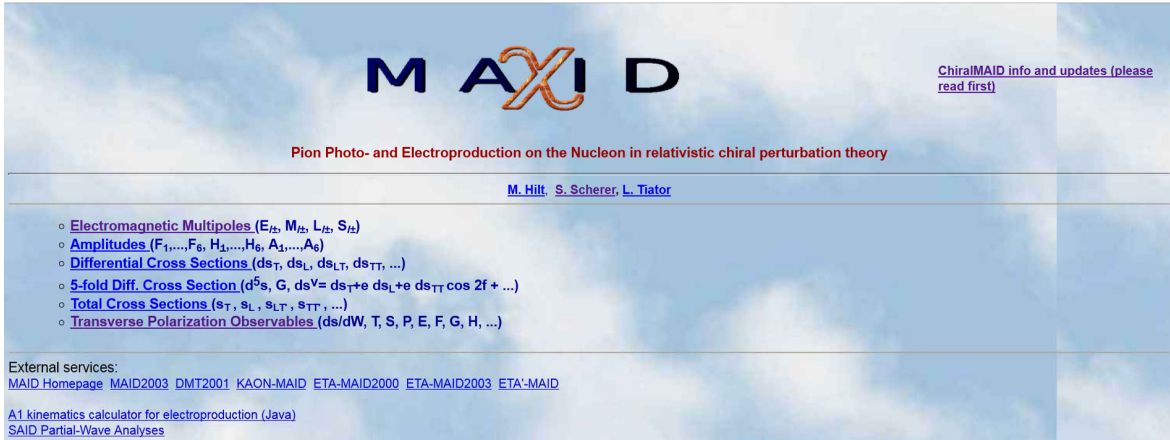


Fig. 2. Chiral MAID homepage [http://www.kph.uni-mainz.de/MAID/chiralmid/].

As a specific example, Fig. 3 shows the settings to calculate the electric dipole amplitude E_{0+} for the physical channels at the real-photon point as a function of the total cm energy W . The corresponding output is shown in Fig. 4. The LECs of the contact interactions can be modified by the user (see Fig. 5). The default settings originate from our fit to the available data (as at year 2013, see Ref. [9]).

Of course, χ MAID has a limited range of applicability. First of all, ChPT without additional dynamical degrees of freedom restricts the energy region, where our results can be applied. In the case

Multipoles

The multipoles can be given in 4 unique sets of isospin or charge channels ([click here for a larger image](#)):

$$\left(A_p^{1/2}, A_n^{1/2}, A^{3/2}\right), \left(A^{1/2}, A^0, A^{3/2}\right), \left(A^0, A^+, A^-\right), \left(A_{\pi^+n}, A_{\pi^-p}, A_{\pi^0p}, A_{\pi^0n}\right)$$

$$A_{\pi^+n} = \sqrt{2}(A^- + A^0) = \sqrt{2}\left(A_p^{1/2} - \frac{1}{3}A^{3/2}\right) = \sqrt{2}\left(A^0 + \frac{1}{3}A^{1/2} - \frac{1}{3}A^{3/2}\right)$$

$$A_{\pi^-p} = -\sqrt{2}(A^- - A^0) = \sqrt{2}\left(A_n^{1/2} + \frac{1}{3}A^{3/2}\right) = \sqrt{2}\left(A^0 - \frac{1}{3}A^{1/2} + \frac{1}{3}A^{3/2}\right)$$

$$A_{\pi^0p} = A^+ + A^0 = A_p^{1/2} + \frac{2}{3}A^{3/2} = A^0 + \frac{1}{3}A^{1/2} + \frac{2}{3}A^{3/2}$$

$$A_{\pi^0n} = A^+ - A^0 = -A_n^{1/2} + \frac{2}{3}A^{3/2} = -A^0 + \frac{1}{3}A^{1/2} + \frac{2}{3}A^{3/2}$$

Further details can be found in D. Drechsel and L. Tiator, J. Phys. G 18 (1992) 449-497. ([scanned version](#))

Type of the multipoles: ☒ (p(1/2), n(1/2), 3/2) ☐ (1/2, 0, 3/2) ☐ (0, +, -) ☐ charge channels

Choose pion angular momentum l : ☒ El+ ☐ El- ☐ Ml+ ☐ Ml- ☐ Ll+ ☐ Ll- ☐ Sl+ ☐ Sl-

Reduced multipoles: ☐

Choose kinematical variables

choose an independent (running) variable: ☐ Q² ☒ W

choose values for Q², W, step size and maximum value:

Q ² (GeV/c) ²	W (MeV)	increment	upper value	click here
<input type="text" value="0"/>	<input type="text" value="1074"/>	<input type="text" value="1"/>	<input type="text" value="1090"/>	<input type="button" value="Calculate"/> <input type="button" value="Reset"/>

Fig. 3. Settings to calculate the electric dipole amplitude E_{0+} for the physical channels.

of neutral pion photoproduction (see Ref. [28]) one can clearly see that for energies above $E_\gamma^{\text{lab}} \approx 170$ MeV the theory starts to deviate from experimental data. The inclusion of the Delta resonance at $O(q^3)$ has recently been discussed in Refs. [29, 30]. In the case of the charged channels the range of applicability is larger, but some observables are quite sensitive to the cutoff of multipoles, as the pion pole term is important at small angles. As an estimate, for $W > 1160$ MeV the difference between our full amplitude and the approximation up to and including G waves becomes visible.

4. Results and Conclusions

In the following, we present two selected results generated with the chiral MAID (see Ref. [9] for a complete discussion). First, in Fig. 6 we show the real parts of the S and P waves of $\gamma + p \rightarrow p + \pi^0$ together with single-energy fits of Ref. [24]. For comparison, we also show the predictions of the Dubna-Mainz-Taipei (DMT) model [31] and the covariant, unitary, chiral approach of Gasparyan and Lutz (GL) [32]. The multipole E_{0+} agrees nicely with the data in the fitted energy range. The reduced P waves $\bar{E}_{1+} = E_{1+}/q_\pi$ and $\bar{M}_{1-} = M_{1-}/q_\pi$ with the pion momentum q_π in the cm frame agree for even higher energies with the single energy fits. The largest deviation can be seen in \bar{M}_{1+} . This multipole is related to the Δ resonance and the rising of the data above 170 MeV can be traced back to the influence of this resonance. As we did not include the Δ explicitly, this calculation is not able to fully describe its impact on the multipole. For electroproduction, $\gamma^* + p \rightarrow p + \pi^0$, in Fig. 7, we show the total cross section $\sigma_{\text{total}} = \sigma_T + \epsilon\sigma_L$ in the threshold region together with the experimental data [33].

In summary we have shown for the first time a chiral perturbation theory approach that can con-

```

C h M A I D 2 0 1 2
M. Hilt, S. Scherer, L. Tiator
Institut fuer Kernphysik, Universitaet Mainz
*****

Pion angular momentum l= 0

All multipoles are given in 10^-3/Mpi+

Q^2 = .000 (GeV/c)^2
*****

.3028 1.2695 .0924 13.2100 e,gA,F[GeV],gpiN=gA*mp/F
-1.0920 -1.2160 4.3370 -4.2600 d8,d9,d20,d21 [GeV^-2]
5.2350 .9250 2.2050 6.6290 -4.1030 -2.6540 e48,e49,e50,e51,e52,e53 [GeV^-3]
-8.2690 -.9250 -1.0350 3.9100 -4.3520 10.5390 2.1200 e67,e68,e69,e70,e71,e72,e73 [GeV^-3]
9.3420-13.7450 e112,e113 [GeV^-3]

W E0+(pi0_p) E0+(pi0_n) E0+(pi+_n) E0+(pi-_p) E(lab) q(cm)
(MeV) Re Im Re Im Re Im Re Im (MeV) (MeV)
1074.00 -1.0608 .0000 2.8400 .0000 27.1931 .0000 -32.7097 .0000 145.54 13.44
1075.00 -.9960 .0000 2.8898 .0000 26.9933 .0000 -32.4886 .0000 146.69 20.45
1076.00 -.9210 .0000 2.9504 .0000 26.7940 .0000 -32.2689 .0000 147.84 25.64
1077.00 -.8301 .0000 3.0279 .0000 26.5939 .0000 -32.0500 .0000 148.98 29.96
1078.00 -.7093 .0000 3.1376 .0000 26.3903 .0000 -31.8308 .0000 150.13 33.75
1079.00 -.4769 .0000 3.3685 .0000 26.1676 .0000 -31.6058 .0000 151.28 37.18
1080.00 -.3758 .3249 3.4564 .3534 25.9705 -.0617 -31.3900 .0215 152.43 40.33
1081.00 -.3959 .4764 3.4121 .5183 25.7986 -.0924 -31.1839 .0331 153.58 43.27
1082.00 -.4162 .5891 3.3672 .6412 25.6292 -.1166 -30.9798 .0430 154.74 46.03
1083.00 -.4367 .6826 3.3218 .7433 25.4625 -.1378 -30.7777 .0521 155.89 48.66
1084.00 -.4573 .7641 3.2758 .8323 25.2982 -.1573 -30.5776 .0609 157.04 51.16
1085.00 -.4780 .8371 3.2293 .9121 25.1364 -.1757 -30.3793 .0696 158.20 53.55
1086.00 -.4989 .9035 3.1822 .9849 24.9770 -.1933 -30.1829 .0782 159.36 55.86
1087.00 -.5199 .9649 3.1346 1.0523 24.8200 -.2104 -29.9883 .0868 160.52 58.08
1088.00 -.5410 1.0221 3.0864 1.1151 24.6654 -.2270 -29.7954 .0955 161.67 60.24
1089.00 -.5623 1.0758 3.0377 1.1741 24.5131 -.2433 -29.6042 .1043 162.83 62.33
1090.00 -.5837 1.1264 2.9884 1.2299 24.3630 -.2593 -29.4147 .1131 164.00 64.36

```

Fig. 4. Output for the electric dipole amplitude E_{0+} for the physical channels.

sistently describe all pion photo- and electroproduction processes in the threshold region equally well. By performing fits to the available experimental data, we determined all 19 LECs of the contact graphs at $O(q^3)$ and $O(q^4)$ (see Table I). Our relativistic chiral perturbation theory calculation is also available online within the MAID project as chiral MAID under <http://www.kph.uni-mainz.de/MAID/>. It is clear that new experiments will lead to different estimates for the LECs [35,36]. For that reason, we included in χ MAID the possibility of changing the LECs arbitrarily. This will help to further study the range of validity and applicability of ChPT in the future.

This work was supported by the Deutsche Forschungsgemeinschaft (SFB 443 and 1044).

References

- [1] E. Mazzucato *et al.*: Phys. Rev. Lett. **57** (1986) 3144
- [2] R. Beck *et al.*: Phys. Rev. Lett. **65** (1990) 1841
- [3] P. De Baenst: Nucl. Phys. **B24** (1970) 633
- [4] A. I. Vainshtein and V. I. Zakharov: Nucl. Phys. **B36** (1972) 589
- [5] S. Scherer and J. H. Koch: Nucl. Phys. **A534** (1991) 461
- [6] V. Bernard, N. Kaiser, J. Gasser, and U.-G. Meißner: Phys. Lett. B **268** (1991) 291
- [7] R. M. Davidson: Phys. Rev. C **47** (1993) 2492
- [8] V. Bernard, N. Kaiser, J. Kambor, and U.-G. Meißner: Nucl. Phys. **B388** (1992) 315
- [9] M. Hilt, B. C. Lehnhart, S. Scherer, and L. Tiator: Phys. Rev. C **88** (2013) 5, 055207
- [10] T. Becher and H. Leutwyler: Eur. Phys. J. C **9** (1999) 643
- [11] J. Gegelia and G. Japaridze: Phys. Rev. D **60** (1999) 114038
- [12] T. Fuchs, J. Gegelia, G. Japaridze, and S. Scherer: Phys. Rev. D **68** (2003) 056005
- [13] Chiral MAID, [<http://www.kph.uni-mainz.de/MAID/chiralmaid/>]

$O(q^3)$ (all couplings in GeV^{-2})						
0		+		-		
d_9		d_8		d_{20}	d_{21}	
-1.216		-1.092		4.337	-4.260	

$O(q^4)$ (all couplings in GeV^{-3})						
Isospin 0						
e_{48}	e_{49}	e_{50}	e_{51}	e_{52}	e_{53}	e_{112}
5.235	0.925	2.205	6.629	-4.103	-2.654	9.342
Isospin +						
e_{67}	e_{68}	e_{69}	e_{71}	e_{72}	e_{73}	e_{113}
-8.269	-0.925	-1.035	-4.352	10.539	2.120	-13.745
Isospin -						
e_{70}						
3.910						

Fig. 5. The LECs of the contact interactions can be modified by the user.

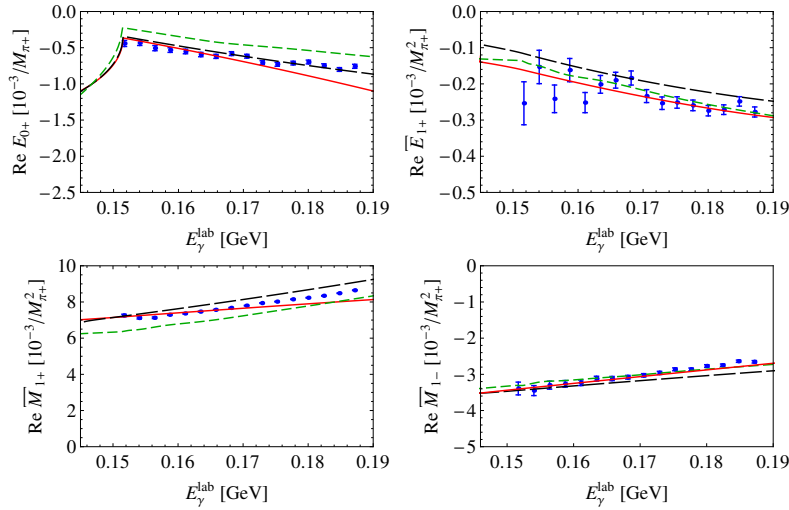


Fig. 6. S - and reduced P -wave multipoles for $\gamma + p \rightarrow p + \pi^0$. The solid (red) curves show our RChPT calculations at $O(q^4)$. The short-dashed (green) and long-dashed (black) curves are the predictions of the DMT model [31] and the GL model [32], respectively. The data are from Ref. [24].

- [14] S. Weinberg: *Physica A* **96** (1979) 327
- [15] J. Gasser and H. Leutwyler: *Annals Phys.* **158** (1984) 142
- [16] J. Gasser, M. E. Sainio, and A. Švarc: *Nucl. Phys.* **B307** (1988) 779
- [17] S. Scherer: *Adv. Nucl. Phys.* **27** (2003) 277
- [18] S. Scherer and M. R. Schindler: *Lect. Notes Phys.* **830** (2012) 1
- [19] J. C. Collins: *Renormalization*, Cambridge University Press, Cambridge, 1984
- [20] S. Weinberg: *The Quantum Theory of Fields. Vol. 1: Foundations*, Cambridge University Press, Cam-

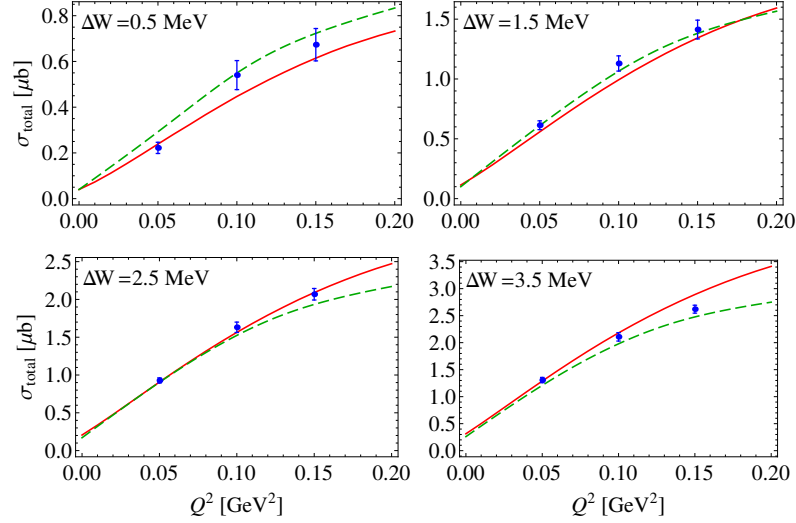


Fig. 7. Total cross sections in μb as a function of Q^2 for different cm energies above threshold ΔW in MeV. The solid (red) curves show our RChPT calculations at $O(q^4)$. The short-dashed (green) curves are the predictions of the DMT model [31]. The data are from Refs. [33].

bridge, 1995

- [21] J. Gegelia, G. S. Japaridze, and K. S. Turashvili: *Theor. Math. Phys.* **101** (1994) 1313 (1994)
- [22] G. F. Chew, M. L. Goldberger, F. E. Low, and Y. Nambu: *Phys. Rev.* **106** (1957) 1345
- [23] P. Denner: *Phys. Rev.* **124** (1961) 2000
- [24] D. Hornidge *et al.* [A2 and CB-TAPS Collaboration]: *Phys. Rev. Lett.* **111** (2013) 062004
- [25] D. Drechsel and L. Tiator: *J. Phys. G* **18** (1992) 449
- [26] R. Mertig, M. Bohm, and A. Denner: *Comput. Phys. Commun.* **64** (1991) 345
- [27] T. Hahn: *Comput. Phys. Commun.* **140** (2001) 418
- [28] M. Hilt, S. Scherer, and L. Tiator: *Phys. Rev. C* **87** (2013) 045204
- [29] A. N. Hiller Blin, T. Ledwig, and M. J. Vicente Vacas: *Phys. Lett. B* **747** (2015) 217
- [30] A. H. Blin, T. Ledwig, and M. V. Vacas: *arXiv:1510.01598* [hep-ph]
- [31] S. S. Kamalov, G.-Y. Chen, S.-N. Yang, D. Drechsel, and L. Tiator: *Phys. Lett. B* **522** (2001) 27
- [32] A. Gasparyan and M. F. M. Lutz: *Nucl. Phys.* **A848** (2010) 126
- [33] H. Merkel: *PoS CD* **09** (2009) 112; H. Merkel *et al.*: *arXiv:1109.5075* [nucl-ex]
- [34] M. Weis *et al.* [A1 Collaboration]: *Eur. Phys. J. A* **38** (2008) 27
- [35] K. Chirapatpimol *et al.* [Hall A Collaboration]: *Phys. Rev. Lett.* **114** (2015) 19, 192503
- [36] I. Frišić: *Measurement of the $p(e,e'\pi^+)n$ reaction with the short-orbit spectrometer at $Q^2 = 0.078$ $(\text{GeV}/c)^2$* , PhD thesis, University of Zagreb, 2015

Table I. Numerical values of all LECs of pion photo- and electroproduction. The * indicates constants that appear in electroproduction, only. If possible, the errors were estimated using the bootstrap method (see Ref. [9] for details). In the case of the electroproduction LECs e_{52} , e_{53} , e_{72} , and e_{73} we can only give errors for $\tilde{e}_{52} = e_{52} + e_{72} = 6.4 \pm 0.7$ and $\tilde{e}_{53} = e_{53} + e_{73} = -0.5 \pm 0.2$.

Isospin channel	LEC	Value
0	d_9 [GeV ⁻²]	-1.22 ± 0.12
0	e_{48} [GeV ⁻³]	5.2 ± 1.4
0	e_{49} [GeV ⁻³]	0.9 ± 2.6
0	e_{50} [GeV ⁻³]	2.2 ± 0.8
0	e_{51} [GeV ⁻³]	6.6 ± 3.6
0	e_{52}^* [GeV ⁻³]	-4.1
0	e_{53}^* [GeV ⁻³]	-2.7
0	e_{112} [GeV ⁻³]	9.3 ± 1.6
+	d_8 [GeV ⁻²]	-1.09 ± 0.12
+	e_{67} [GeV ⁻³]	-8.3 ± 1.5
+	e_{68} [GeV ⁻³]	-0.9 ± 2.6
+	e_{69} [GeV ⁻³]	-1.0 ± 2.2
+	e_{71} [GeV ⁻³]	-4.4 ± 3.7
+	e_{72}^* [GeV ⁻³]	10.5
+	e_{73}^* [GeV ⁻³]	2.1
+	e_{113} [GeV ⁻³]	-13.7 ± 2.6
-	d_{20} [GeV ⁻²]	4.34 ± 0.08
-	d_{21} [GeV ⁻²]	-3.1 ± 0.1
-	e_{70} [GeV ⁻³]	3.9 ± 0.3